



Multiple traces and altered signal-to-noise in systems consolidation: Evidence from the 7T fMRI Natural Scenes Dataset

Thomas J. Vanasse^a, Melanie Boly^a, Emily J. Allen^{b,c}, Yihan Wu^d, Thomas Naselaris^e, Kendrick Kay^b, Chiara Cirelli^a, and Giulio Tononi^{a,1}

Edited by Lynn Nadel, The University of Arizona, Tucson, AZ; received January 31, 2022; accepted May 18, 2022

The brain mechanisms of memory consolidation remain elusive. Here, we examine blood-oxygen-level-dependent (BOLD) correlates of image recognition through the scope of multiple influential systems consolidation theories. We utilize the longitudinal Natural Scenes Dataset, a 7-Tesla functional magnetic resonance imaging human study in which ~135,000 trials of image recognition were conducted over the span of a year among eight subjects. We find that early- and late-stage image recognition associates with both medial temporal lobe (MTL) and visual cortex when evaluating regional activations and a multivariate classifier. Supporting multiple-trace theory (MTT), parts of the MTL activation time course show remarkable fit to a 20-y-old MTT time-dynamical model predicting early trace intensity increases and slight subsequent interference ($R^2 > 0.90$). These findings contrast a simplistic, yet common, view that memory traces are transferred from MTL to cortex. Next, we test the hypothesis that the MTL trace signature of memory consolidation should also reflect synaptic “desaturation,” as evidenced by an increased signal-to-noise ratio. We find that the magnitude of relative BOLD enhancement among surviving memories is positively linked to the rate of removal (i.e., forgetting) of competing traces. Moreover, an image-feature and time interaction of MTL and visual cortex functional connectivity suggests that consolidation mechanisms improve the specificity of a distributed trace. These neurobiological effects do not replicate on a shorter timescale (within a session), implicating a prolonged, offline process. While recognition can potentially involve cognitive processes outside of memory retrieval (e.g., re-encoding), our work largely favors MTT and desaturation as perhaps complementary consolidative memory mechanisms.

memory consolidation | multiple-trace theory | fMRI

Systems consolidation refers to the reorganization of a memory trace with prolonged time and experience across large-scale neuronal networks (1). The precise mechanisms underlying this process remain unclear, but the end result includes the stabilization of certain memories, the equally vital forgetting of nonessential information (2), and the transformation of some memories into more behaviorally adaptive or gist-like representations (3). Influential theories of systems-level consolidation are largely built upon the seminal observations that varying medial temporal lobe (MTL) damage causes an inverse memory effect, whereby the ability to recall recently encoded memories is reduced while many older memories (weeks to years) remain intact (4).

Theoretical approaches to explain these findings began with the standard consolidation theory (SCT), which proposed that MTL contributions to any memory trace diminish over time (5). Alternatively, multiple-trace theory (MTT), put forward in 1997, clarified inconsistencies of this standpoint with many experiments showing that MTL lesions caused more severe retrograde amnesia for episodic than for semantic memories (6, 7). For example, Bright et al. (8) showed limited retrograde amnesia for a variety of tests of public events and personalities (semantic memory), while for autobiographical episodes, a retrograde amnesia extended back further. Episodic memories contain elements often in the form of visual images (9) that are recollected within some overlaying context (10). MTT posited that an episodic memory must rely on the MTL, and on multiple content-relevant cortical modules, across its entire lifespan, not just the beginning. Early MTT developments emphasized that episodic memory reactivations—which occur during conscious recall or recognition but also during “offline” memory replays (11) within waking quiescence and sleep (12, 13)—lead to a rich distributed network of multiple, overlaid traces in the MTL over time. This process, coined as “trace expansion,” would presumably provide memory protection from partial lesions (14). Within the human functional magnetic resonance imaging (fMRI) literature, there are conflicting reports (14) showing both SCT-predicted decreases in

Significance

How do the neural correlates of recognition change over time? We study natural scene image recognition spanning a year with 7-Tesla functional magnetic resonance imaging (fMRI) of the human brain. We find that the medial temporal lobe (MTL) contribution to recognition persists over 200 d, supporting multiple-trace theory and contradicting a trace transfer (from MTL to cortex) point of view. We then test the hypothesis that the signal-to-noise ratio of traces increases over time, presumably a consequence of synaptic “desaturation” in the weeks following learning. The fMRI trace signature associates with the rate of removal of competing traces and reflects a time-related enhancement of image-feature selectivity. We conclude that multiple MTL traces and improved signal-to-noise may underlie systems-level memory consolidation.

Author contributions: T.J.V., E.J.A., Y.W., T.N., and K.K. designed research; T.J.V., E.J.A., Y.W., T.N., and K.K. performed research; T.J.V. contributed new analytic tools; T.J.V., M.B., C.C., and G.T. analyzed data; and T.J.V., M.B., C.C., and G.T. wrote the paper.

The authors declare no competing interest.

This article is a PNAS Direct Submission.

Copyright © 2022 the Author(s). Published by PNAS. This article is distributed under [Creative Commons Attribution-NonCommercial-NoDerivatives License 4.0 \(CC BY-NC-ND\)](https://creativecommons.org/licenses/by-nc-nd/4.0/).

¹To whom correspondence may be addressed. Email: gtononi@wisc.edu.

This article contains supporting information online at <http://www.pnas.org/lookup/suppl/doi:10.1073/pnas.2123426119/-DCSupplemental>.

Published October 24, 2022.

hippocampus activity during recall (e.g., refs. 15–17) and MTT-predicted increases in hippocampus activity during recall (e.g., refs. 18–20). Most of this prior work has a limited time perspective (with only three or fewer timepoints), and brain measurements were not acquired with high-field fMRI. Moreover, while multiple time-dynamical analytic models of MTL trace intensity have been inspired by the nonlinear probability time curves of retrograde amnesia (21), to our knowledge, there has not yet been any application of these mathematical formulations to functional human neuroimaging data due to the paucity of timepoints and samples.

The analysis of the connectivity between the MTL and the neocortex offers a crucial perspective of systems-level memory consolidation (3). Intracranial human studies are now establishing precise timing links between the hippocampus and content-relevant cortex necessary for memory retrieval (22–26). For instance, Norman et al. (26) investigated autobiographical memory remoteness spanning days, weeks, and months. They demonstrated that hippocampal ripples—high-frequency (~80 to 100 Hz in humans) oscillatory events in hippocampal local field potentials—correlate with memory remoteness and promote communication across large-scale networks. According to the authors, their findings “support theories that emphasize richer hippocampal representations of remote memories (e.g., the MTT)” (26), which conflicts with SCT. SCT emphasizes that the MTL’s role should be diminished over time. While SCT does not posit that MTL traces are entirely removed, a simplistic but common narrative derives itself from SCT: fully consolidated memories (episodic or semantic) may completely lose their dependency on the hippocampus (12, 27, 28), which we refer to hereon as “trace transfer.” The validity of these viewpoints—MTT, SCT, and trace transfer—remains unclear.

Mechanistic underpinnings of systems consolidation may rely on an increased signal-to-noise ratio of traces, although this has not been explicitly addressed by either SCT or MTT. Specifically, because most learning involves strengthening synaptic connections throughout the brain, intense learning is poised to increase cellular needs for energy and supplies, move synapses close to saturation, and decrease signal-to-noise ratios (2). Sleep is the principal mechanism that renormalizes net synaptic strength and restores cellular homeostasis while maintaining certain memory traces (2, 29). In this regard, retaining memories—through sleep or other consolidation mechanisms—may result in the reorganization of the synaptic landscape to promote desaturation and, thus, improve signal-to-noise ratios of surviving traces at the systems level. Simulation models and recent studies in mice have, indeed, supported this perspective (30–32). However, more evidence is necessary to advance this hypothesis.

Here, we utilize the recently acquired, publicly available Natural Scenes Dataset (NSD), an unprecedented resource to study memory consolidation (33). Over 300 d, eight subjects participated in weekly 7-Tesla (7T) fMRI scans while exposed to the NSD; ~135,000 trials (~2/3 of total trials) involved subjects seeing an image that was previously presented in the experiment. We first examined the relevant memory consolidation models in describing trace evolution. Does natural scene image recognition, which we presume to be episodic in nature, continually rely on the MTL over time as MTT suggests, or are these traces transferred to cortex as suggested by the trace transfer thesis? Furthermore, in regard to MTT, can MTL time dynamics be explained by a precise mathematical model formulated in the early MTT literature? And can the timescale (days vs. min) of trace evolution be distinguished from different mathematical frameworks? In the latter part of this work, we

investigated the hypothesis that increased signal-to-noise ratio of brain traces would occur over time. Specifically, we tested whether the relative blood-oxygen-level-dependent (BOLD) enhancement of surviving traces over time is linked to the concomitant deletion of other traces (i.e., forgetting). Finally, because the MTL is proposed to bind content-relevant cortical modules, we assessed whether the specific MTL connectivity changes according to specific image-feature content.

Results

Data Volume and Memory Performance. The NSD experiment used ultra-high-field fMRI (7T, whole-brain, T_2^* -weighted gradient-echo echo-planar imaging, 1.8-mm resolution, 1.6-s repetition time) to acquire BOLD responses in each of eight participants who viewed 9,000 to 10,000 distinct, color natural scenes (22,500–30,000 trials) in 30 to 40 weekly scan sessions over the course of a year. In each scan session, 750 images were shown. A trial here is defined as one 4-s image presentation (3-s image presentation followed by 1-s fixation). Images were from Microsoft’s Common Objects in Context image database (<https://www.cocodataset.org>). As participants fixated a central point, they performed a continuous recognition task in which they judged whether they had seen each image at any time during the experiment, either in the current scan session or in any previous scan session (Fig. 1A). Hereon, “rep0” designates a trial where a novel image was shown, and “rep1” and “rep2” designate repetition trials upon their second and third presentations, respectively. Most repetitions (rep1/rep2) were acquired in sessions and trials that were temporally near a preceding presentation (Fig. 1B and C); the exact placement of all trials was chosen according to a mixture of a von Mises and uniform distribution (see ref. 33).

The NSD demonstrates that not only could subjects accurately recognize images within a session (average = 90.69% hit rate), but their recognition also persisted over an extended period of time. In Fig. 1C, we plot the adjusted hit rate, which is the hit rate (rate of rep1/rep2 remembered) minus the false positive rate (rate of rep0 images identified as old, plotted for reference) over 10-d windows. The adjusted hit rate for rep1 and rep2 images remains above 0, even at 200 d. While the volume of applicable repetition trials decreases as the time window from the previous repetition gets longer, there still are ample samples even at the 200- to 210-d time window: $n = 714$ rep1, $n = 496$ rep2 trials. While the NSD maximum distance extended for 300 d, our analysis was limited to 210 d because the adjusted hit rate rapidly approached 0 after this timepoint (in addition to smaller sample size). For an extended discussion of the memory metrics of this NSD, see Allen et al. (33).

MTL Activation during Recognition Increases over Time, in Support of MTT. For this study, anatomical regions of interest (ROIs) included the most commonly considered parcels of the MTL: the hippocampus proper (HP), parahippocampal cortex (PhC), perirhinal cortex (PrC), and entorhinal cortex (ErC) (Fig. 2A). Because of a broad literature supporting a differential long axis of the HP (34), we split HP into anterior and posterior portions.

We first assessed whether the MTL activation significantly increased over time among recognized images, which MTT would suggest under the assumption that BOLD activation can indeed be used as a proxy for “trace density.” We compared activations per each MTL region between within-session image recognition (day 0) and outside-session (>day 0) recognition among successful

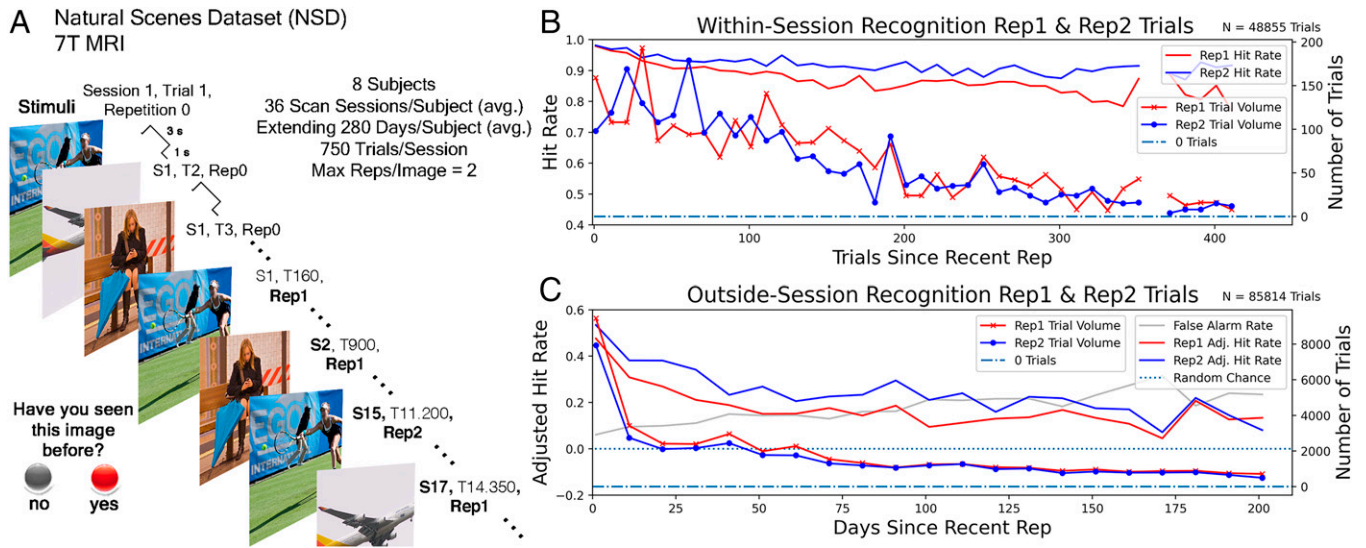


Fig. 1. NSD: stimuli, hit rates, and data volume. (A) Example of image presentations and their repetition “rep1” (image previously seen once) or “rep2” (image previously seen twice) designations. For each 4-s trial, each subject was asked whether they had seen the image before. (B) Unmarked lines on top (y axis, left) show the within-session hit rate (i.e., proportion of repetition images recognized), which remains high (average = 91%). Red crosses and blue circles mark the number of trials across subjects at that specific timepoint (binned every 10 d) for rep 1 and rep2, respectively (y axis, right). Time since last image repetition (rep1 minus rep0 or rep2 minus rep1) is on the x axis in trials. (C) Unmarked lines on top (y axis, left) show adjusted hit rate (hit rate - false positive rate), where random guessing would result in an adjusted hit rate of 0 (dashed line). Red crosses and blue circles mark the number of trials across subjects at that specific timepoint (binned every 10 d) for rep1 and rep2, respectively (y axis, right). Time since last image repetition (rep1 – rep0 or rep2 – rep1) over extended time period (1 to 200 d).

rep1 and rep2 trials. We, indeed, found that outside-session image recognition activation was significantly greater in each MTL parcel besides the posterior HP (Bonferroni-corrected $P < 0.05$) (Fig. 2B). Upon further separating the data among each subject, we

found that medium effect sizes were present in PhC and PrC ($d \sim 0.3$), while small effect sizes were present in the anterior HP and ErC ($d \sim 0.1$) (Fig. 2C). To further characterize these increases, we plotted the activation time course of each parcel with

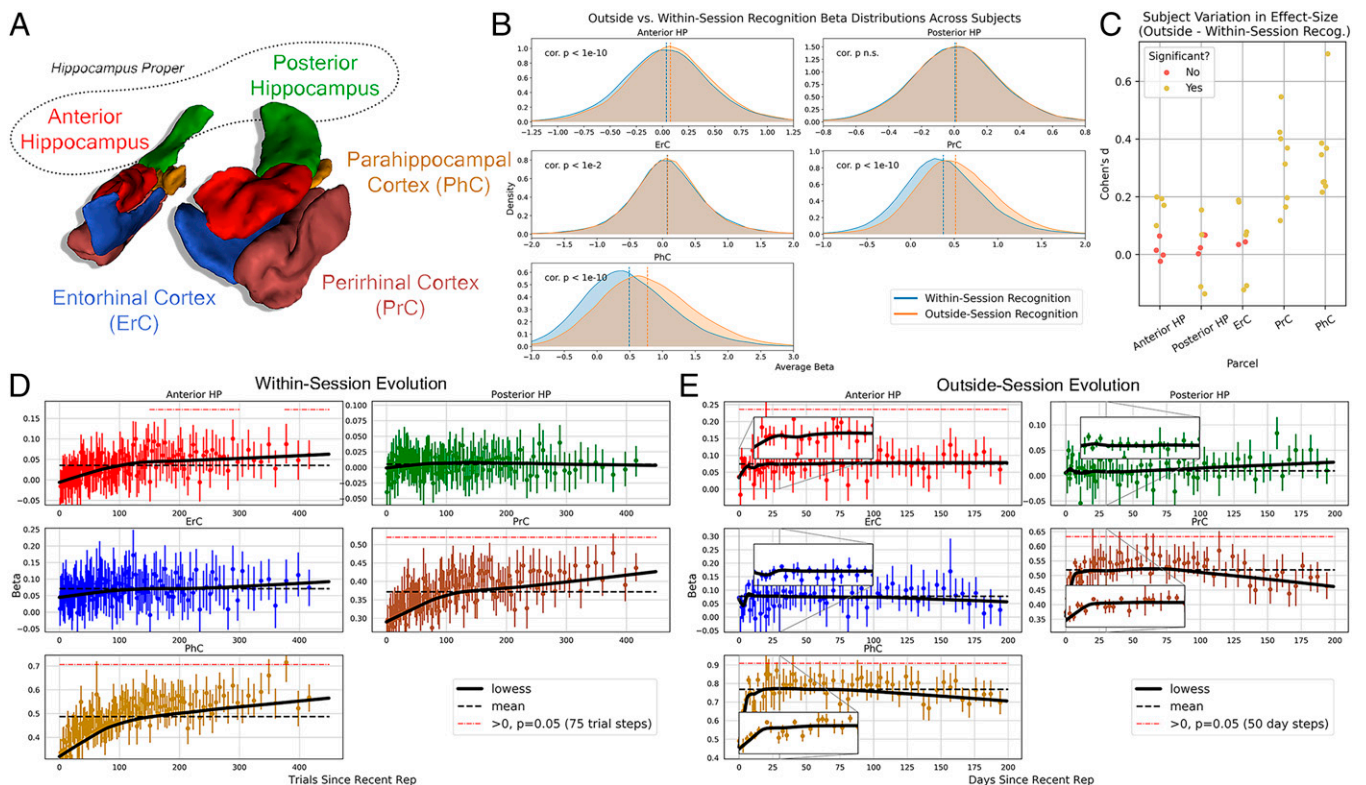


Fig. 2. MTL ROIs and outside- vs. within-session recognition differences in activation/evolution. (A) MTL ROIs identified with ASHS tool in one subject. (B) Activation (percent increase in BOLD signal after image presentation) differences between within-session and outside-session recognition conditions, per MTL ROI, along with associated P value and effect size. (C) Differences in effect size among outside- minus within-session recognition among subjects. Significance corresponds to Bonferroni-corrected $P < 0.05$. (Bottom) Evolution of activation across trials, within-session (D), and across days, outside-session (E). LOWESS is shown in black, and the mean is shown with a dotted line. Only correctly recognized rep1/rep2 trials are shown. Error estimates on scatterplots are 95% bootstrap CIs.

locally weighted scatterplot smoothing (LOWESS) plots (Fig. 2D and E).

Classifier Model Shows MTL and Cortex Remain Steady across Time. To investigate changes in brain regions' contributions to recognition over time, we applied a multivariate classifier model of BOLD activations to predict successful versus unsuccessful recognition. This pattern analysis approach allowed us to quantify sets of brain regions that optimally contributed to image recognition, with the goal of comparing trace transfer (i.e., decreasing MTL and increasing visual contributions with time) and MTT models (i.e., maintenance or increase of MTL and visual contributions over time). A multivariate logistic regression classifier was applied with the MTL and visual sets on their own and in combination (5, 25, and 30 ROIs, respectively) in outside- versus within-session recognition (Fig. 3A). We report the cross-validation balanced accuracy in classifying hit vs. miss responses among rep1 images. To simplify any interpretations, we focused on rep1 images for this and all following analyses (Figs. 3–6), which do not incorporate “reconsolidation” effects. The trace transfer model would assume that MTL would be most predictive of recognition early (with little to no contribution from the visual system [VS]), and the VS would be most predictive of recognition later, with little to no contribution from the MTL.

The trace contributions between early and late recognition were not significantly different—neither the main effect of session (within vs. outside; $F = 3.0$, $P = 0.12$) nor the session \times ROI interaction ($F = 1.3$, $P = 0.29$). The main effect of ROI combinations (BOLD activations within MTL, VS, and MTL + VS sets) was highly significant ($F = 46.8$, $P < 0.0001$): for the outside-session recognition condition (Fig. 3B), the 25 visual ROIs and the 5 MTL ROIs in combination showed the best mean balanced accuracy at 59.6%. This was significantly better than the VS (58.6%), at a P (corrected) of 0.027. The MTL showed 56.4% balanced accuracy. Early recognition (within-session) accuracies included the MTL + VS (63.1%), VS (61.9%), and MTL (58.2%). We also provide a supplementary analysis separating early memory, intermediate memory, and later-stage memory, which did not alter our

initial conclusion since there was no significant effect across timepoints (SI Appendix, Fig. S5).

Time-Dynamical Modeling Further Corroborates MTT. We next evaluated the time evolution of MTL activation with two time-dynamical models. The first model we test is derived according to MTT principles (Fig. 4A). The second model is the memory-chain model (35). The latter model is most representative of trace transfer, as it hypothesizes a complete trace transfer from a lower-level store to a higher-level store (from working memory neural systems to the MTL, or from MTL to neocortical system).

The MTT model by Nadel and colleagues (21) assumed that 1) MTL traces expand over time, 2) this expansion rate decays with time (with a preferential effect on more recent memories to expand as opposed to older memories), and 3) these traces are vulnerable to natural degradation or interference (replacement with newer traces). The multiple-trace model that was applied to the BOLD data here is provided below (Eq. 1):

$$TI_1 = e^{\kappa(\tau-t)} + e^{\frac{\sigma}{\alpha} - \kappa t} \alpha \int_{\frac{\sigma}{\alpha}}^{\frac{t}{\sigma}} dx \frac{x^{\kappa\sigma-1}}{x-1} \quad [1]$$

Parameters referenced here include trace intensity TI_1 , the average intensity of traces per memory at time stamp τ ; κ is the constant interference rate; α is the total replication rate, which is constant; and σ quantifies the replication rate decay function, which decreases exponentially with memory age.

The memory-chain model (35) assumes that memory representations in a store decline in strength while trying to induce new representations in higher-level, more permanent stores; one process induces another, more permanent process. The memory-chain model can potentially be applicable to either the within-session (short) or outside-session (long) timescales. A complete removal of the early store gives the following “relative-retrograde” curve where only the late-store can contribute to a memory:

$$TI_2 = c \left[\frac{-a_1(1 - e^{a_1 t})^{-1}}{\mu_2} + 1 \right]^{-1} \quad [2]$$

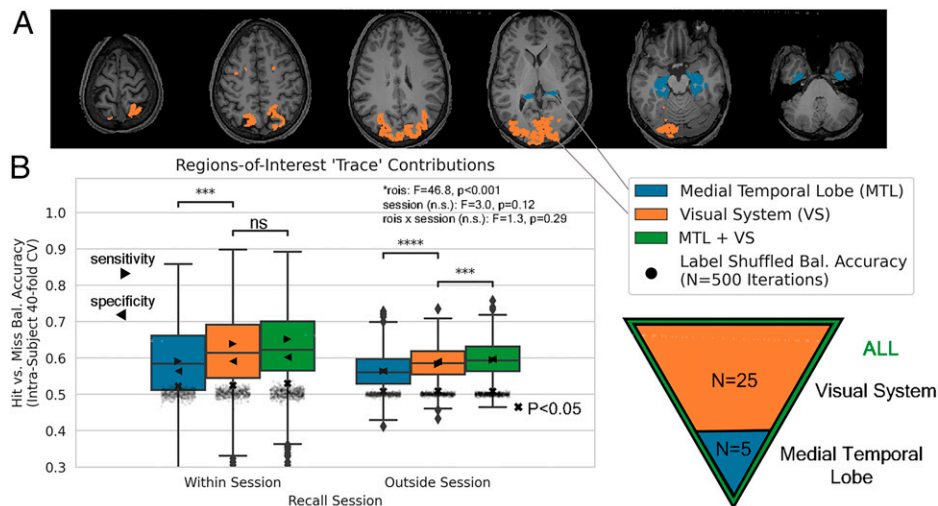


Fig. 3. Early- and late-trace contributions from ROI activation patterns. (A) ROI activations used as features in classifier analysis (from subject 1). Colors correspond to combined $n = 5$ MTL parcels and $n = 25$ VS (Kastner Atlas) designations. (B) Recognition success was tested per subject on rep1 images by using a logistic regression model with a combination of ROI feature sets. Training/testing cross validation was done per subject. Marked “x”s show significance ($P < 0.05$) pertaining to distribution of balanced accuracy (average of sensitivity and specificity, also plotted) of 500 iterations of shuffled labels. $n = 25,753$ early (within-session) rep1 image samples and $n = 46,091$ late (outside-session) rep1 image samples were collected. MTL included 5 ASHS ROIs, and VS included 25 Kastner Atlas ROIs; in combination (“ALL”), there were 30 distinct ROIs. Boxes/whiskers entail 25th to 75th and 5th to 95th percentiles.

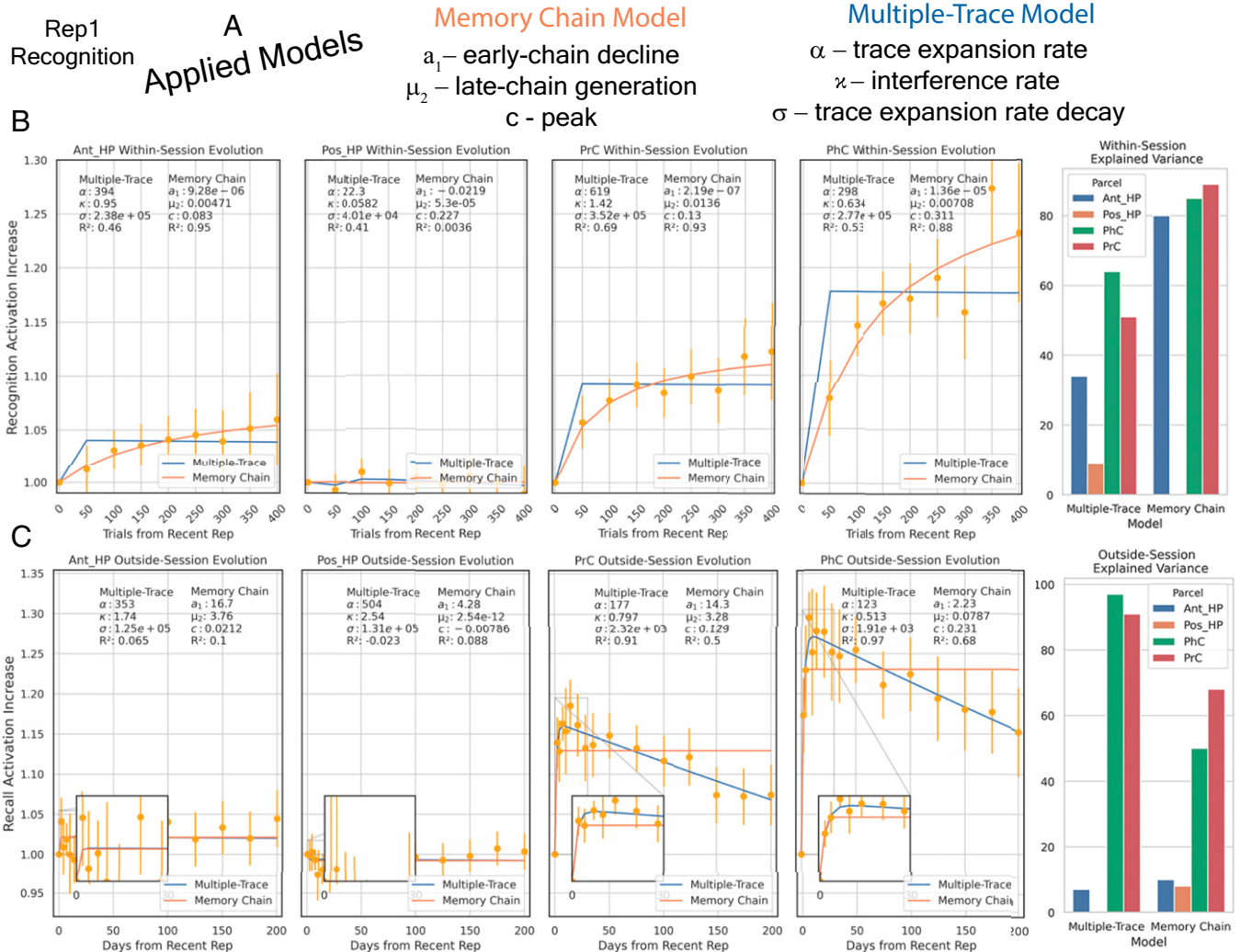


Fig. 4. Memory-chain model fits within-session while multiple-trace model fits outside-session MTL evolution. (A) Summary of variables within each model. (B and C) Each model is fit to PhC/PrC neural activation evolution among (B) within-session and (C) outside-session activation evolution along with a labeling of associated variables. Analytic model fit to rep1 neural activation data upon recognition (increases were assessed by parameter estimates from dummy encoding time bins). (Right) Explained variance from each corresponding model per MTL ROI. Neural activation was uniformly shifted along the y axis so that the mean of activation at day 0 (within-session recognition) was in accordance with each model's initial condition. Error bars represent 95% CIs of parameter estimate.

Here, a_1 represents the early-chain decline, and a_2 is the late-chain decline. μ_1 and μ_2 are the early-chain and late-chain growth parameters, respectively. c is a constant that marks the height of the asymptote.

Both neurobiological models were fit to MTL activations in the within-session (Fig. 4B) and outside-session (Fig. 4C) timescales. The memory-chain model showed strong fits to the within-session timescale: anterior hippocampus $R^2 = 0.8$, PrC $R^2 = 0.93$, and PhC $R^2 = 0.88$. The multiple-trace model showed poor within-session fits: anterior hippocampus $R^2 = 0.34$, PrC $R^2 = 0.64$, and PhC $R^2 = 0.51$. However, this model performance shifted when analyzing the outside-session timescale. The multiple-trace model here showed an excellent outside-session fit: $R^2 = 0.97$ and $R^2 = 0.91$ in PhC and PrC, respectively, compared to the memory-chain model ($R^2 = 0.68$ and $R^2 = 0.50$).

As hypothesized, the outside-session timescale was fit well by the MTT mathematical model. While a separate memory-chain mathematical model explained outside-session evolution quite well, which is valuable in its own right, it could not explain the prolonged evolution of memory traces as well as MTT. Using a

least-squares optimizer from the lmfit Python package (36) to obtain Bayesian information criteria (BIC), we indeed found better PrC/PhC multiple-trace model versus memory-chain model fits for outside-session evolution (PrC/PhC BIC = $-129/-133$ vs. $-102/-95.9$, respectively).

Does Increased Signal-to-Noise Ratio Underlie Relative BOLD Enhancement? To investigate the hypothesis that an increase in signal-to-noise ratios underlies trace consolidation with time, we tested for a potential association between change in memory performance (forgetting) and the increase in MTL activation upon recognition. Specifically, we hypothesized that the increased rate of forgetting here should represent reduced noise among those surviving memories, which should, thus, translate to a stronger averaged BOLD signal among the surviving memory traces.

In computing the subject-specific derivative of memory recognition across sessions (hit rate), we found considerable variation across subjects. Still, the peak of the memory loss rate usually occurred at around 5 d, and the derivative stabilized at around 15 to 20 d (Fig. 5A). Crucially, we found that the peak forgetting

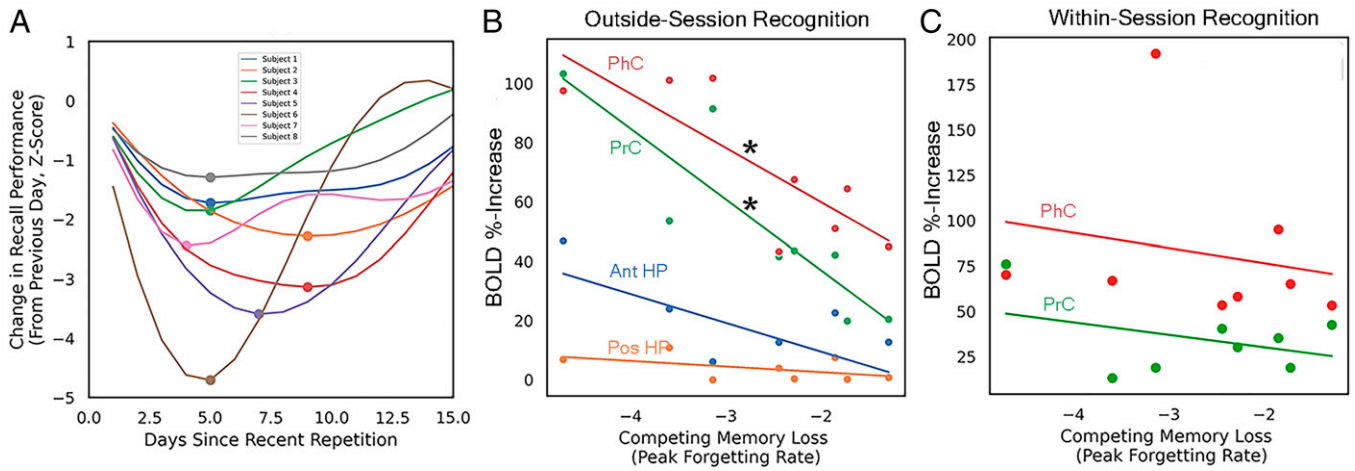


Fig. 5. Overall forgetting rate associates with MTL BOLD signature of surviving memory traces across individuals. (A) The derivative of the smoothed “forgetting curve” [remembered trials/(remembered + forgotten trials)] for each subject across 1 to 15 d since the previous image repetition for rep1 presentations. Circles designate the peak forgetting rate for each subject, which occurs at around 5 to 9 d and eventually stabilizes at around 15 to 20 d. Derivative is z-scored from 0 to 250 d data. (B) Scatterplots showing the correlations between competing memory loss (x axis) and surviving memory BOLD increase (y axis) for each subject among the anterior HP, posterior HP, PrC, and PhC. PrC and PhC fits were significant, corresponding to P corrected < 0.05 . BOLD percent increase corresponds to changes from average within-session recognition to peak of curve fit (via MTT model) per subject (see Fig. 3). (C) As a control analysis, the peak outside-session rep1 forgetting rate was also correlated with the within-session BOLD increases among the PrC/PhC parcels (increased BOLD at trial 350; y axis). No significant association was found.

rate of rep1 images significantly correlated with the peak increase in MTL activation of surviving memory traces (i.e., those correctly recognized) within the PrC ($r = -0.88$, Bonferroni-corrected $P = 0.008$) and PhC ($r = -0.82$, Bonferroni-corrected $P = 0.02$; Fig. 5B). Anterior HP ($r = -0.71$) and posterior HP ($r = -0.51$) were not significant. Furthermore, when we tested the association of the outside-session rep1 peak forgetting rate with the increases in PrC/PhC BOLD activation of rep1 trials within a session, we did not find any significant effect (Fig. 5C).

Changes in Connectivity for Feature-Specific Recognition over Time. We next tested whether specific features of the images modulated changes in MTL connectivity. Thus, we asked whether changes in MTL connectivity to neocortex were dependent on the type of image recognized. We focused on face images and confined this connectivity analysis to the specialized occipital face area (OFA) and two fusiform face areas (FFA1 and FFA2) as provided by the NSD project for each subject. This line of results was more focused on image features since the MTL serves to bind specific, content-relevant cortical modules (23). We had *a priori* interest in the PrC as a “seed” because of its selectivity to faces and object memory (37, 38). Using the cortical face areas as separate dependent variables, we performed a three-way (seed \times time \times face) interaction test with a linear mixed-effects model (Fig. 6) to test whether the decline in connectivity differed between face images, which can be considered the “signal,” and no-face (noise) images in these regions.

The strongest interaction effect for each face-selective region peaked within a window of 1 to 20 d since the most recent image presentation. The interaction peak effect was strongest in the OFA ($\beta_{OFA,interaction} = 0.025 \pm 0.013$, $P = 0.0001$), but the other face-selective regions were also significant ($\beta_{FFA1,interaction} = 0.019 \pm 0.012$, $P = 0.002$; $\beta_{FFA2,interaction} = 0.019 \pm 0.01$, $P = 0.005$). These interactions were further investigated *post hoc* by calculating the correlations within the session of interest and face versus no-face groupings at the peak magnitude of the interaction effect (trials 1 to 20 d since the recent image presentation). This analysis suggested that the interaction effect was driven by a more significant decrease in connectivity in nonface image recognition over time (Fig. 6).

To evaluate the specificity of this effect to the outside-session timescale (i.e., across days), we also applied the same connectivity analysis to the short within-session timescale (i.e., across trials). There was no significant (Bonferroni $P < 0.05$) seed \times time \times face interaction on the within-session timescale (*SI Appendix, Fig. S4*) in the PrC-OFA, PrC-FFA1, or PrC-FFA2 connectivity.

Discussion

In this work, we used the recently released NSD to test either MTT or trace transfer in understanding systems consolidation. We employ “trace transfer” to represent a more simplistic narrative of SCT, where MTL traces are thought to perhaps entirely transfer from MTL to cortex. Specifically, we found that increased MTL activity is associated with recognition at both early and late timepoints. The time-dynamical properties of the MTL suggest that surviving traces become more robust in the weeks after encoding and persist over extended periods of time (>200 d) with slight decline. Our classifier analysis also demonstrated that both the MTL and visual cortex supported image recognition at early and late timepoints, which distinctly contrasts with the concept of trace transfer. Furthermore, the PrC and PhC outside-session evolution showed an excellent fit to an early mathematical model of MTL trace strength by Nadel et al. (21).

The applied MTT time-dynamical model is based on the idea that episodic memories expand their traces within the MTL over time upon repeated reactivations (21) or implicit/offline reactivations (10). This process is thought to offer a protective effect to partial MTL damage, whereby any intact trace could contribute to successful recognition if others are lost. Extrahippocampal MTL structures (PhC and PrC) showed the strongest evidence for increased activation across sessions, yet the anterior HP and ErC still demonstrated a small but significant groupwise effect of increased activation when considering outside-session versus within-session recognition. This small but significant effect in anterior HP should be emphasized, as it relies on the vast sample size, timescale, and high-field resolution of the current experiment. Perhaps related to shortcomings among those attributes, one recent

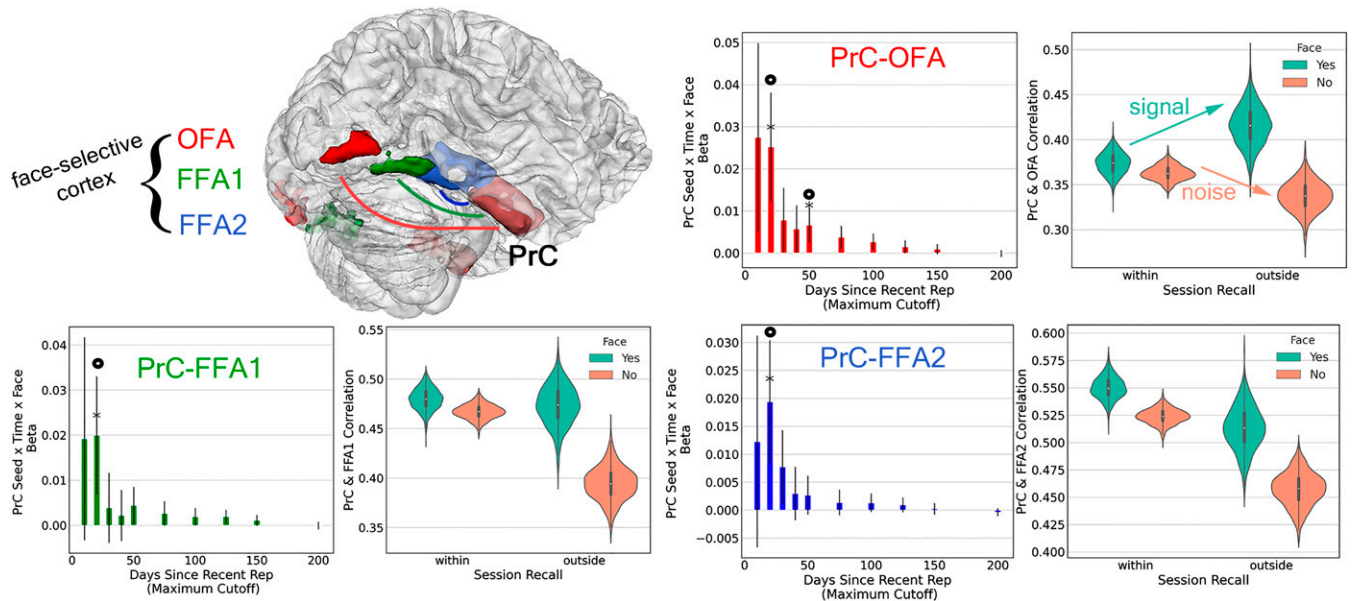


Fig. 6. Feature-specific MTL connectivity time evolutions: OFA in red, FFA1 and FFA2 in green and blue, and PrC defined within a given subject. Seed \times time (days) \times face interaction beta estimates for each MTL ROI designation within a linear mixed-effects model, where OFA activation was the dependent variable. Betas were calculated across various timepoint cutoffs since the last image presentation (10, 20, 30, 40, 50 ... 200). The 95% CIs of beta estimates are displayed, and a circle/asterisk denotes significance at $P < 0.05$, corrected. Correlations of each condition of interest are shown where trials were cut off to recent repetitions of 20 d or less. Distribution corresponds to correlations derived from $n = 1,000$ bootstrap resamples with replacement. Only correct rep1 trials were considered.

image recognition experiment did not find such a significant effect using the entire hippocampus as an ROI (14). While there are difficulties in interpreting the BOLD activations only with respect to memory retrieval, as opposed to other cognitive processes (see *Limitations*), these results may indeed reflect a richer trace contribution of the MTL over time. Lesions in extrahippocampal MTL regions (PrC/PhC/ErC) have, indeed, been implicated in more severe amnesia when compared to damage restricted to HP (35, 39). And while there are undoubtedly functional intricacies and interactions within the MTL, from our understanding, the early work of SCT (40) and MTT (21) lumped together the PrC, ErC, PhC, and HP for their model formulations. We believe this to be a useful dichotomy (MTL vs. cortex), which guided our analyses here.

The precise fit of the MTT time-dynamical model to the outside-session activation data is remarkable when considering that it was formulated roughly 20 y ago. The separate memory-chain model did not perform nearly as well on the outside-session timescale as the multiple-trace model. However, the memory-chain model did perform well on the within-session timescale. This model presupposes that a rapidly declining initial chain (assumed here to be cortical areas involved in working memory) is transferring traces to a more permanent chain (assumed here to be MTL). In summary, the shift of model performance from the short to long timescales suggests that a differential mechanistic process is, indeed, occurring for systems-level (i.e., outside-session) transformations.

A classifier model to predict image recognition via a multivariate pattern analysis provided more evidence against trace transfer. Specifically, the results of this analysis do not indicate a representational transfer from MTL to the neocortex (specifically, visual cortex) for natural scene image recognition. Instead, trace contributions (as measured by predictive ability to discriminate successful recognition) from the VS and MTL occur at both early and late timepoints. Our classifier analysis also showed the best accuracy for the MTL and visual cortex in

combination and only at outside-session recognition. This may be another indicator of improved specificity in MTL and visual cortex connectivity (among a backdrop of decreased connectivity for the broader MTL and visual cortex) that resulted in better predictive capability of recognition.

The significant association between the magnitude of overall memory decline and increased PrC/PhC activation among remembered rep1 trials (across subjects) is interesting to consider in the context of trace expansion. While trace “replicas” may, indeed, be instantiated with time as initially proposed, we offer evidence that a growing signal-to-noise ratio (i.e., reduced noise over time) in the MTL may be a complementary factor (30) supporting memory consolidation. In other words, as many memory traces with similar “time stamps” degrade at a rapid rate, the neural signature of the intact ones could expand accordingly because of the reduction of interference/noise by competing traces. The relative increases in BOLD responses over those days may, thus, result from the preservation of some traces in the context of a net decrease in synaptic strength during that time or from the formation of multiple traces (2).

Functional connectivity of the cortex with the hippocampus is known to increase when events are remembered as opposed to forgotten (41). In support of a role of the hippocampus to “bind” disparate cortical modules (42), recent work found that distinct internetwork connections of the MTL (perirhinal and parahippocampal aspects) with neocortical areas, indeed, tracked the precision of remembering certain episodic memory aspects by their item-feature or spatial-context quality (43). A content-general connectivity analysis (*SI Appendix, Fig. S2*) shows broad decreases in MTL-VS connectivity upon recognition over time. This analysis appears to be more in line with SCT predictions of “fast-changing” MTL-VS diminishing connections to potentially be replaced with slower cortico-cortical connections. Furthermore, we do not know to what extent that image recognition here may be transitioning from an episodic to a semantic representation over time (which both theories

allow). One possibility is that the decrease in MTL BOLD activity after the peak—which MTT describes as a decreasing trace-replication rate combined with interference—may allow for semantic representations to form in cortical representations, which SCT emphasizes. Future work may shed more light on this question.

While the positive effects of sleep on memory consolidation and integration are well established, the underlying mechanisms remain highly debated. According to the synaptic homeostasis hypothesis, sleep allows a renormalization of synaptic weights after learning has led to a net increase in synaptic strength, a claim supported by molecular, ultrastructural, and electrophysiological evidence (2, 29). Renormalization keeps the high energy costs of synaptic activity under control and avoids synaptic saturation. It also promotes memory consolidation by increasing the signal-to-noise ratio, because sleep-dependent synaptic weakening is hypothesized to be selective and affords relative protection to the synapses engaged by new learning. Supporting this idea, a recent study found that sleep promotes the consolidation of a motor skill by broadly weakening synapses that did not potentiate during encoding, thus providing a relative advantage to the “learned” synapses (32). Another proposed mechanism for sleep-dependent memory consolidation is the further strengthening, during sleep, of the synaptic connections potentiated by learning (13, 44). This process is thought to occur by the sequential reactivation of specific neurons and synapses during cortical slow oscillations and hippocampal sharp-wave ripples (45–47). The current experiment was not designed to test whether the offline consolidation of some memories occurred during sleep or wake, but an obvious difference between within- and outside-session recognition is that multiple sessions are separated by several days, which include multiple episodes of sleep. We found that the peak forgetting rate of rep1 images was correlated with the peak increase in MTL activation of surviving memory traces. Furthermore, while there were widespread decreases in recognition-related connectivity over time between MTL and visual cortex, specific functional connections relevant to image features (faces) remained resilient as compared to no-face images. Like the correlation between peak forgetting rate and BOLD activation of surviving memory traces, the interaction between time and feature-related connectivity was present over the weeks following the encoding of successfully recognized images but not over minutes and hours within the encoding session. Therefore, the successful recognition of some images depended on the forgetting rate of all other images over weeks but not within a single session. Similarly, the successful recognition of face images was associated with a decline in functional connectivity between MTL and cortical face areas over weeks but not within a single session, and this decline was mainly driven by the no-face images. This offline, long-term (across sessions) effect may reflect feature-irrelevant “noise removal” among the surviving, distributed traces. The OFA encodes low-level image-based properties, while FFA1/2 encode complex social traits (48). We assume MTL connectivity to these cortical modules is necessarily maintained for face recognition at the expense of MTL connectivity to those same cortical modules during recognition of scene images without faces.

In principle, an increase in the signal-to-noise ratio is compatible both with synaptic down-selection (2, 29) and with sleep-dependent synaptic strengthening (13, 44). On the other hand, the finding that BOLD activation of surviving memory traces was correlated with peak forgetting rate may be more in line with the idea that sleep serves to maintain overall synaptic strength, which requires protecting some synapses at the expense

of others. In summary, the qualitative difference between memory consolidation within and outside sessions suggests that factors other than simple passage of time may be involved. Whether sleep is one such factor, as well as the underlying mechanisms, will require direct experimental tests.

Limitations. We interpret changes in brain activity upon image recognition over time as associated with retrieval-related, recollection processes (or “trace density”) to compare memory theories. However, there are other cognitive processes occurring simultaneously to retrieval that are likely contributing to the BOLD signal. These include 1) cognitive effort (i.e., task difficulty), 2) familiarity as opposed to recollection, and 3) re-encoding. Regarding cognitive effort, our reported PrC/PhC MTL time-evolution curves do not reflect a simple linear increase to ultimate peak, as might be expected when considering only task difficulty. Instead, this curve is parabolic, which MTT concisely parameterizes with trace “growth rate,” “growth rate decrease,” and “interference.” With familiarity, the present analysis did not employ the common “remember versus know” study paradigm (49, 50), which treats recognition confidence as a proxy of episodic versus semantic memory systems. The inferotemporal cortex and even PrC have been previously implicated in image familiarity detection, but the direction of such modulation in the PrC is unclear (51). In one item-recognition task by Ritchey et al. (50), no significant difference was found in anterior HP, PrC, and PhC activity via a recollection versus familiarity contrast in either immediate or delayed timepoints. Finally, re-encoding likely occurred during repetition trials, and its impact on the analyzed BOLD signal is unknown. The combination of these factors must be considered while interpreting the current results.

Materials and Methods

We analyzed data from the NSD, which is freely available at [natural-scenes-dataset.org](https://www.natural-scenes-dataset.org). The eight participants included two males and six females, with an age range of 19 to 32 y (see *SI Appendix, Table S1*). The starting point for all analyses in this work were the version 3 betas “b3” as shared through the NSD project. These betas correspond to the percent BOLD signal change (relative to the blank image presented) before the image stimulus. We provide a basic explanation of b3 betas in *SI Appendix*, and an exhaustive explanation regarding the b3 extraction can be found in the original data paper (33).

ROIs. All analyses included ROIs, where betas were averaged over that space: 5 MTL regions, 25 VS regions, and 3 specialized face cortex regions. The automated segmentation of the hippocampus (ASHS) tool (*ashes-fastahs_2.0.0*) was applied using the Institute of Cognitive Neurology and Dementia Research Magdeburg Young Adult 7T Atlas (52) to segment the MTL into bilateral anterior hippocampus (ant hp), bilateral posterior hippocampus (pos hp), bilateral ErC, bilateral PrC, and bilateral PhC. Anterior/posterior hippocampus were separated at $y = -27$ (Montreal Neurological Institute reference).

When investigating the VS (Fig. 3 and 6), 25 ROIs were utilized from the Kastner Atlas (53). Three face ROIs (utilized in Fig. 6) were derived per subject through the NSD *fLoc* experiment (separate from the continuous recognition NSD experiment). These ROIs included the OFA and two FFAs (FFA1, FFA2). In a supplementary analysis, the Yeo17 network parcel was also used (54).

Outside- vs. Within-Session Recognition. In Fig. 2*B, D*, and *E*, raw betas are shown to display the percentage BOLD activation per trial. Correctly recognized, rep1/rep2 trials were extracted from all sessions. A linear logistic regression classifier was applied to different groups of features (MTL, VS, MTL + VS). Only rep1 trials were considered, and only the betas were further grouped (per session) to be standardized before analysis. Models were trained within each subject according to a randomly shuffled k-fold (inner = 20 splits; outer = 40 splits) nested cross-validation procedure (via `sklearn's cross_val_score` method). Mean

balanced accuracy, grand averaged across sessions and subjects, was applied as our metric of interest. Differences in balanced accuracies between feature sets were identified with a mixed-effects model accounting for random intercepts of subjects. A difference among balanced accuracies was tested with a two-way, repeated measures ANOVA (using a mean aggregate function per subject). Each sample here corresponds to the balanced accuracy of one cross-validation fold, and there were 40 folds per subject. Because feature groupings were found to be significantly different in the ANOVA, *post hoc* differences were then assessed between feature groupings (e.g., within-session MTL vs. within-session VS).

Memory Model Fits. Using eight simple assumptions, the MIT model (21) is based on the following first-order differential (Eq. 3) and initial condition (Eq. 4):

$$\frac{\partial}{\partial t} \mu(\tau, t) + \kappa \mu(\tau, t) = \alpha \theta(t - \tau) \frac{\rho(\mu, \tau, t)}{Z([\mu], t)} + \delta(t - \tau) \quad [3]$$

$$\mu(\tau, 0) = 0 \quad [4]$$

Furthermore, their primary model assumed an exponential decrease in trace formation rate with memory age (Eq 5):

$$\rho(\mu, \tau, t) = e^{-\frac{t-\tau}{\sigma}} \quad [5]$$

Parameters referenced here include μ , the mean number of traces per memory at time stamp τ ; t corresponds to the total timepoints in the model; κ is the constant forgetting rate that can be interpreted as the total trace formation rate times the probability that a newly created trace will destroy a given trace by interference; α is the total replication rate, which is constant; ρ is the replication rate decay function, which decreases; Z is a normalization constant; θ is a heaviside step function; and δ is the Kronecker delta.

The memory-chain model is derived from a two-process intensity model:

$$r_{12} = \mu_1 e^{-a_1 t} + \frac{\mu_1 \mu_2}{a_1 - a_2} (e^{-a_2 t} - e^{-a_1 t}) \quad [6]$$

Here, a_1 represents the early-chain decline, and a_2 is the late-chain decline. μ_1 and μ_2 are the early-chain and late-chain growth parameters, respectively. Of note, a_2 is assumed to be much larger than a_1 and, thus, was taken to be zero in Eq. 2.

Mean changes in *repl1* beta activation since time after the last image presentation were extracted by encoding dummy variables (days since most recent image presentation) in a linear mixed-effects model. For Fig. 5, the MIT model was fit to the outside-session data per subject. The percent increase was

calculated based on the peak of the model fit. More information is provided in *SI Appendix*. Furthermore, in a supplementary analysis, we investigated potential shifts in signal “baseline” across sessions (*SI Appendix*). Toward this end, we regressed out the session-of-recognition variable. Our findings and interpretations remained consistent after this procedure.

Connectivity. A seed \times time \times face interaction was assessed with a linear mixed-effects model. Trials included in the model varied with a maximum cutoff of days since most recent image repetition and were tested at max days of 10, 20, 30, 40, 50, 75, 100, 125, 150, and 200. The number of trials per category that powered this analysis is provided in *SI Appendix, Table S3*, which provides evidence against any potential bias due to sample size. No interaction effect remained significant when the analysis was limited to images that were not successfully recognized. A content-general connectivity analysis was also applied between all MTL and VS ROIs (*SI Appendix, Fig. S2*) and is described in *SI Appendix*.

Code Availability. The NSD is freely available to the public. More information about the NSD can be found at www.naturalscenesdataset.org/. Open-source Python packages were utilized for all analyses and are detailed in *SI Appendix*. Furthermore, we feature our code implementation in *SI Appendix*.

Data Availability. All code is shared in the *SI Appendix*.

ACKNOWLEDGMENTS. Research reported in this publication was supported by the National Institute of Neurological Disorders and Stroke of the NIH under Award F32NS114034. Collection of the NSD was supported by NSF IIS-1822683 (K.K.) and NSF IIS-1822929 (T.N.). G.T., C.C., and M.B. are supported by a grant from the Tiny Blue Dot Foundation and the Department of Defense (G.T. and C.C., W911NF1910280). The content herein is solely the responsibility of the authors and does not necessarily represent the official views of the funding organizations.

1. S. McKenzie, H. Eichenbaum, Consolidation and reconsolidation: Two lives of memories? *Neuron* **71**, 224–233 (2011).
2. G. Tononi, C. Cirelli, Sleep and the price of plasticity: From synaptic and cellular homeostasis to memory consolidation and integration. *Neuron* **81**, 12–34 (2014).
3. E. T. Cowan, A. C. Schapiro, J. E. Dunsmoor, V. P. Murty, Memory consolidation as an adaptive process. *Psychon. Bull. Rev.* **28**, 1796–1810 (2021).
4. W. B. Scoville, B. Milner, Loss of recent memory after bilateral hippocampal lesions. *J. Neurol. Neurosurg. Psychiatry* **20**, 11–21 (1957).
5. L. R. Squire, Memory and the hippocampus: A synthesis from findings with rats, monkeys, and humans. *Psychol. Rev.* **99**, 195–231 (1992).
6. L. Nadel, M. Moscovitch, Memory consolidation, retrograde amnesia and the hippocampal complex. *Curr. Opin. Neurobiol.* **7**, 217–227 (1997).
7. G. Winocur, M. Moscovitch, Memory transformation and systems consolidation. *J. Int. Neuropsychol. Soc.* **17**, 766–780 (2011).
8. P. Bright *et al.*, Retrograde amnesia in patients with hippocampal, medial temporal, temporal lobe, or frontal pathology. *Learn. Mem.* **13**, 545–557 (2006).
9. M. A. Conway, Episodic memories. *Neuropsychologia* **47**, 2305–2313 (2009).
10. M. J. Sekeres, G. Winocur, M. Moscovitch, The hippocampus and related neocortical structures in memory transformation. *Neurosci. Lett.* **680**, 39–53 (2018).
11. G. Findlay, G. Tononi, C. Cirelli, The evolving view of replay and its functions in wake and sleep. *Sleep Adv.* **1**, zpab002 (2021).
12. J. G. Klinzing, N. Niethard, J. Born, Mechanisms of systems memory consolidation during sleep. *Nat. Neurosci.* **22**, 1598–1610 (2019).
13. B. Rasch, J. Born, About sleep’s role in memory. *Physiol. Rev.* **93**, 681–766 (2013).
14. C. W. Tallman, R. E. Clark, C. N. Smith, Human brain activity and functional connectivity as memories age from one hour to one month. *Cogn. Neurosci.*, 10.1080/17588928.2021.2021164. (2022).
15. L. C. Dandolo, L. Schwabe, Time-dependent memory transformation along the hippocampal anterior-posterior axis. *Nat. Commun.* **9**, 1–11 (2018).
16. X. Du *et al.*, Differential activation of the medial temporal lobe during item and associative memory across time. *Neuropsychologia* **135**, 107252 (2019).
17. O. Furman, A. Mendelsohn, Y. Dudai, The episodic engram transformed: Time reduces retrieval-related brain activity but correlates it with memory accuracy. *Learn. Mem.* **19**, 575–587 (2012).
18. S. Bosshardt *et al.*, One month of human memory consolidation enhances retrieval-related hippocampal activity. *Hippocampus* **15**, 1026–1040 (2005).

Author affiliations: ^aCenter for Sleep and Consciousness, Department of Psychiatry, University of Wisconsin-Madison, Madison, WI 53719; ^bCenter for Magnetic Resonance Research (CMRR), Department of Radiology, University of Minnesota, Minneapolis, MN 55455; ^cDepartment of Psychology, University of Minnesota, Minneapolis, MN 55455; ^dGraduate Program in Cognitive Science, University of Minnesota, Minneapolis, MN 55455; and ^eDepartment of Neuroscience, University of Minnesota, Minneapolis, MN 55455

19. S. Gais *et al.*, Sleep transforms the cerebral trace of declarative memories. *Proc. Natl. Acad. Sci. U.S.A.* **104**, 18778–18783 (2007).
20. J. F. Smith *et al.*, Imaging systems level consolidation of novel associate memories: A longitudinal neuroimaging study. *Neuroimage* **50**, 826–836 (2010).
21. L. Nadel, A. Samsonovich, L. Ryan, M. Moscovitch, Multiple trace theory of human memory: Computational, neuroimaging, and neuropsychological results. *Hippocampus* **10**, 352–368 (2000).
22. D. Pacheco Estefan *et al.*, Coordinated representational reinstatement in the human hippocampus and lateral temporal cortex during episodic memory retrieval. *Nat. Commun.* **10**, 2255 (2019).
23. Y. Norman *et al.*, Hippocampal sharp-wave ripples linked to visual episodic recollection in humans. *Science* **365**, eaax1030 (2019).
24. A. P. Vaz, S. K. Inati, N. Brunel, K. A. Zaghloul, Coupled ripple oscillations between the medial temporal lobe and neocortex retrieve human memory. *Science* **363**, 975–978 (2019).
25. A. P. Vaz, J. H. Wittig, Jr, S. K. Inati, K. A. Zaghloul, Replay of cortical spiking sequences during human memory retrieval. *Science* **367**, 1131–1134 (2020).
26. Y. Norman, O. Raccah, S. Liu, J. Parvizi, R. Malach, Hippocampal ripples and their coordinated dialogue with the default mode network during recent and remote recollection. *Neuron* **109**, 2767–2780.e5 (2021).
27. X. Liu, D. Kuzum, Hippocampal-cortical memory trace transfer and reactivation through cell-specific stimulus and spontaneous background noise. *Front. Comput. Neurosci.* **13**, 67 (2019).
28. S. Diekelmann, J. Born, The memory function of sleep. *Nat. Rev. Neurosci.* **11**, 114–126 (2010).
29. G. Tononi, C. Cirelli, Sleep and synaptic down-selection. *Eur. J. Neurosci.* **110**, 3101 (2019).
30. A. T. Nere, A. Hashmi, C. Cirelli, G. Tononi, Sleep-dependent synaptic down-selection (I): Modeling the benefits of sleep on memory consolidation and integration. *Front. Neurol.* **4**, 143 (2013).
31. A. Hashmi, A. Nere, G. Tononi, Sleep-dependent synaptic down-selection (II): Single-neuron level benefits for matching, selectivity, and specificity. *Front. Neurol.* **4**, 148 (2013).
32. D. Miyamoto, W. Marshall, G. Tononi, C. Cirelli, Net decrease in spine-surface GluA1-containing AMPA receptors after post-learning sleep in the adult mouse cortex. *Nat. Commun.* **12**, 2881 (2021).
33. E. J. Allen *et al.*, A massive 7T fMRI dataset to bridge cognitive neuroscience and artificial intelligence. *Nat. Neurosci.* **25**, 116–126 (2022).
34. J. Poppenk, H. R. Eversmoen, M. Moscovitch, L. Nadel, Long-axis specialization of the human hippocampus. *Trends Cogn. Sci.* **17**, 230–240 (2013).
35. J. M. J. Murre, A. G. Chessa, M. Meeter, A mathematical model of forgetting and amnesia. *Front. Psychol.* **4**, 76 (2013).
36. M. Newville, T. Stensitzki, D. B. Allen, A. Ingargiola, LMFIT: Non-linear least-square minimization and curve-fitting for Python (0.8.0). *Zenodo*, <https://zenodo.org/record/11813#YnTRLnMJ6o> (2014). Accessed 1 March 2022.

37. M. E. Mundy, P. E. Downing, D. M. Dwyer, R. C. Honey, K. S. Graham, A critical role for the hippocampus and perirhinal cortex in perceptual learning of scenes and faces: Complementary findings from amnesia and fMRI. *J. Neurosci.* **33**, 10490–10502 (2013).
38. B. P. Staresina, J. Fell, A. T. Do Lam, N. Axmacher, R. N. Henson, Memory signals are temporally dissociated in and across human hippocampus and perirhinal cortex. *Nat. Neurosci.* **15**, 1167–1173 (2012).
39. P. J. Bayley, R. O. Hopkins, L. R. Squire, The fate of old memories after medial temporal lobe damage. *J. Neurosci.* **26**, 13311–13317 (2006).
40. P. Alvarez, L. R. Squire, Memory consolidation and the medial temporal lobe: A simple network model. *Proc. Natl. Acad. Sci. U.S.A.* **91**, 7041–7045 (1994).
41. B. R. Geib, M. L. Stanley, N. A. Dennis, M. G. Woldorff, R. Cabeza, From hippocampus to whole-brain: The role of integrative processing in episodic memory retrieval. *Hum. Brain Mapp.* **38**, 2242–2259 (2017).
42. B. Mišić, J. Goñi, R. F. Betzel, O. Sporns, A. R. McIntosh, A network convergence zone in the hippocampus. *PLoS Comput. Biol.* **10**, e1003982 (2014).
43. R. A. Cooper, M. Ritchey, Cortico-hippocampal network connections support the multidimensional quality of episodic memory. *eLife* **8**, 709 (2019).
44. M. G. Frank, R. Cantera, Sleep, clocks, and synaptic plasticity. *Trends Neurosci.* **37**, 491–501 (2014).
45. B. E. Pfeiffer, The content of hippocampal "replay". *Hippocampus* **30**, 6–18 (2020).
46. H. R. Joo, L. M. Frank, The hippocampal sharp wave-ripple in memory retrieval for immediate use and consolidation. *Nat. Rev. Neurosci.* **19**, 744–757 (2018).
47. B. Giri, H. Miyawaki, K. Mizuseki, S. Cheng, K. Diba, Hippocampal reactivation extends for several hours following novel experience. *J. Neurosci.* **39**, 866–875 (2019).
48. M. Tsantani *et al.*, FFA and OFA encode distinct types of face identity information. *J. Neurosci.* **41**, 1952–1969 (2021).
49. C. Harand *et al.*, The hippocampus remains activated over the long term for the retrieval of truly episodic memories. *PLoS One* **7**, e43495 (2012).
50. M. Ritchey, M. E. Montchal, A. P. Yonelinas, C. Ranganath, Delay-dependent contributions of medial temporal lobe regions to episodic memory retrieval. *eLife* **4**, e05025 (2015).
51. T. Meyer, N. C. Rust, Single-exposure visual memory judgments are reflected in inferotemporal cortex. *eLife* **7**, e32259 (2018).
52. D. Berron *et al.*, A protocol for manual segmentation of medial temporal lobe subregions in 7 Tesla MRI. *Neuroimage Clin.* **15**, 466–482 (2017).
53. L. Wang, R. E. B. Mruzczek, M. J. Arcaro, S. Kastner, Probabilistic maps of visual topography in human cortex. *Cereb. Cortex* **25**, 3911–3931 (2015).
54. B. T. T. Yeo *et al.*, The organization of the human cerebral cortex estimated by intrinsic functional connectivity. *J. Neurophysiol.* **106**, 1125–1165 (2011).